Available online at www.sciencedirect.com

ScienceDirect

Mendeleev Commun., 2024, **34**, 18–21

Mendeleev Communications

Doxorubicin delivery systems based on polypeptide nanoparticles for subcutaneous administration in cancer therapy

Natalia N. Sudareva,[a,b] Irina I. Tarasenko,[a] Dmitry N. Suslov,[c] Olga M. Suvorova,[a] Konstantin A. Kolbe,[a] Galina Y. Yukina,[b] Margarita L. Tyndyk,[c] Yulia G. Zmitrichenko[c] and Evgenia G. Korzhikova-Vlakh*[a,d]

[a] *Institute of Macromolecular Compounds, Russian Academy of Sciences, 199004 St. Petersburg, Russian Federation. E-mail: vlakh@hq.macro.ru*
[b] *I. P. Pavlov First St. Petersburg Medical University, 197002 St. Petersburg, Russian Federation*
[c] *N. N. Petrov National Medical Research Center of Oncology, 197758 St. Petersburg, Russian Federation*
[d] *Institute of Chemistry, St. Petersburg State University, 198584 St. Petersburg, Russian Federation*

DOI: 10.1016/j.mencom.2024.01.006

Polypeptide-based doxorubicin delivery systems were prepared and their physicochemical and functional properties, such as size, encapsulation efficiency, stability, release of doxorubicin in various media and cytotoxicity, were characterized. An *in vivo* study revealed an effective reduction of tumor growth when these systems were administered subcutaneously.

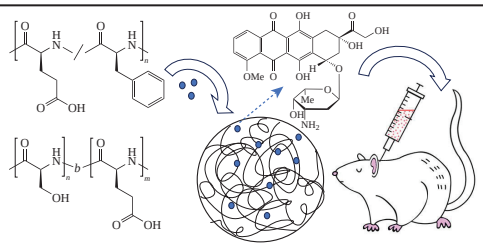

Keywords: doxorubicin, synthetic polypeptides, nanoparticles, delivery systems, cancer treatment, subcutaneous administration.

Cancer still remains one of the leading causes of death in the world. Approximately 19–20 million people are diagnosed with cancer annually, of whom 10 million die each year.[1] One of the most common types of cancer is breast cancer, affecting one in eight women.[2]

Doxorubicin (DOX) is a powerful broad-spectrum anthracycline antibiotic that inhibits the growth of tumors, including solid breast tumors. The action of DOX is based on DNA damage through intercalation.[3] The high efficacy of DOX is accompanied by dose-dependent systemic toxicity and rapid elimination from the body.[4] With recent advances, nanoscale delivery systems loaded with anticancer drugs are increasingly being considered for cancer treatment.[5] However, sometimes nanoscale systems, even in non-cytotoxic concentrations, have negative effects on body cells.[6]

The main modern requirements for nanoscale delivery systems for anticancer drugs, including DOX, are improved bioavailability, reduced toxicity and sustained release.[5,7] To achieve sustained release of the drug into the bloodstream as well as reduce systemic toxicity, various DOX delivery systems have been developed in recent decades.[5,8–11] There are currently a number of commercially available liposomal and PEGylated liposomal systems for the delivery of DOX.[12] For instance, liposomal formulations include Myocet (Elan Pharma, USA), Lipodox (Bharat Seram, India) and Doxyl (Janssen, Belgium), while Caelyx (TTY Biopharm, Taiwan) is based on PEGylated liposomes. Although liposomal DOX delivery systems are used in clinics, the main drawbacks of liposomes are their low stability in the bloodstream and lack of sustained release. Recently, HPLC was used to determine the levels of DOX released from different delivery systems at different time points in the plasma of healthy female outbred rats.[13] It has been shown that after intraperitoneal injection of 4 mg of encapsulated DOX to rats, it is detectable in the blood for up to 21 days. At the same time, free DOX administered in the same way is eliminated from the body after 3 days.

In this work, we developed nanoscale DOX formulations based on random and block copolymers of a polypeptide nature, evaluated the loading and release rate of the drug, cytotoxicity *in vitro* and also studied the developed formulations *in vivo* under subcutaneous administration. Unlike intravenous or intraperitoneal administration, subcutaneous administration ensures slow penetration of DOX into the bloodstream due to the poorly developed network of blood vessels in the subcutaneous adipose layer. However, free DOX is known to cause local tissue damage and necrosis when administered subcutaneously and intramuscularly.[14] In turn, subcutaneous administration of encapsulated DOX may minimize this side effect and at the same time create a drug depot to ensure a sustained therapeutic effect.

Recently, nanoparticles based on poly(L-glutamic acid-*co*-L/D-phenylalanine) have been studied *in vitro* as potential delivery systems for various peptide drugs.[15–17] Here we used self-assembled nanoparticles based on poly(L-glutamic acid-*co*-D-phenylalanine) [P(Glu-*co*-Phe)] and poly-L-serine-*b*-poly(L-glutamic acid) (PSer-*b*-PGlu) for the preparation of DOX nanoformulations. Both copolymers were synthesized by ring-opening polymerization of *N*-carboxyanhydrides of the corresponding amino acids using *n*-hexylamine as an initiator. During the synthesis of P(Glu-*co*-Phe), the [Glu]/[Phe] ratio in the polymerization mixture was four. In the synthesis of PSer-*b*-PGlu, PSer was first synthesized and then used as a macroinitiator for PGlu. In all cases, the ratio of monomer(s) to (macro)initiator was 50. For details on the polymerization and purification of the copolymers, see Online Supplementary Materials. The structure of the copolymers was confirmed by ^{1}H NMR spectroscopy (Figure S1, see Online Supplementary Materials). The molecular weight (M_w), dispersity ($Đ$) and composition (monomer ratio) of the copolymers were determined by size-exclusion chromatography and reversed-phase HPLC analysis of free amino acids obtained after total acid hydrolysis of polypeptides (Figures S2, S3 and Table S1,

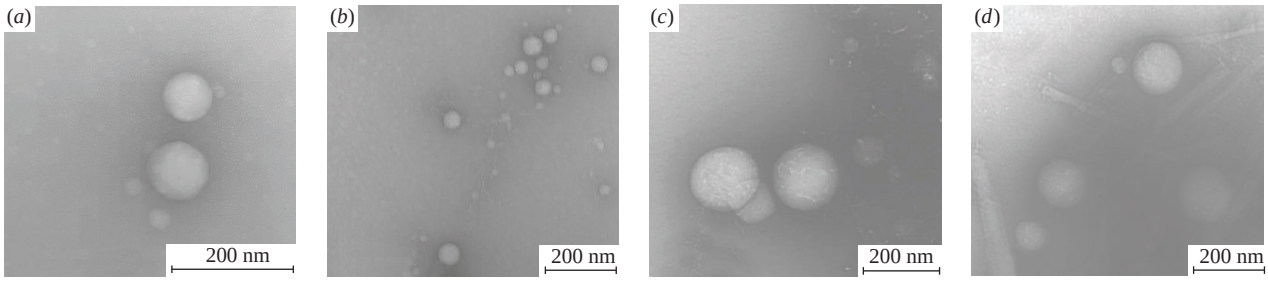

Figure 1 TEM images of polypeptide nanoparticles of different composition: (*a*) P(Glu-*co*-Phe), (*b*) P(Glu-*co*-Phe)/DOX, (*c*) PSer-*b*-PGlu and (*d*) PSer-*b*-PGlu/DOX.

Table 1 Physicochemical characteristics of empty nanoparticles and DOX nanoformulations determined in the dry state (TEM, 22 °C) and aqueous media (DLS, ELS, 25 °C).

Polymer nanoparticles	Medium	TEM	DLS		ELS
		$\bar{D}$/nm	D_H/nm	PDI	ζ potential/mV
P(Glu-*co*-Phe)	PBS (pH 7.4)	90 ± 32	168	0.19	–50.0 ± 0.2
P(Glu-*co*-Phe)	H_2O	–	188	0.25	–
PSer-*b*-PGlu	PBS (pH 7.4)	116 ± 56	295	0.24	–27.7 ± 0.9
PSer-*b*-PGlu	H_2O	–	189	0.22	–
P(Glu-*co*-Phe)/DOX[a]	PBS (pH 7.4)	59 ± 41	130	0.34	–44.5 ± 0.2
PSer-*b*-PGlu/DOX[b]	PBS (pH 7.4)	179 ± 51	270	0.38	–20.1 ± 0.8

[a] The sample contains 459 ± 15 μg of DOX per 1 mg of P(Glu-*co*-Phe). [b] The sample contains 490 ± 10 μg of DOX per 1 mg of PSer-*b*-PGlu.

see Online Supplementary Materials). The synthesized copolymers have the following characteristics: M_w = 6500, $Đ$ = 1.28 and [Glu]/[Phe] = 2.9 for P(Glu-*co*-Phe) and M_w = 7750, $Đ$ = 1.21 and [Glu]/[Ser] = 1.6 for PSer-*b*-PGlu.

Both copolymers in an aqueous medium are capable of self-organization into soft spherical nanoparticles (Figure 1). Since both polypeptides were synthesized using *n*-hexylamine as an initiator, each copolymer chain has a terminal C_6 aliphatic tail, which may also contribute to self-assembly.† In the case of amphiphilic P(Glu-*co*-Phe), the driving force for self-organization is hydrophobic interactions between Phe units and the hexyl tails of different macromolecules. In turn, the more hydrophilic PSer-*b*-PGlu forms nanoparticles due to hydrophobic interactions of the hexyl tails at the initial stage. Afterwards, the nanoparticles may additionally be stabilized by hydrogen bonds between the carboxyl groups of Glu and the hydroxyl groups of Ser. The characteristics of the nanoparticles determined from transmission electron microscopy (TEM) images and measured by dynamic and electrophoretic light scattering (DLS/ELS) methods are presented in Table 1. For details on sample preparation and characterization, see Online Supplementary Materials.

The average hydrodynamic diameter (D_H) of P(Glu-*co*-Phe) in buffer solution is lower than that of PSer-*b*-PGlu nanoparticles, while their hydrodynamic diameters in water are the same. Moreover, the hydrodynamic diameter for P(Glu-*co*-Phe) is almost independent of the redispersion medium, which can be explained by the high stabilization of nanoparticles due to hydrophobic interactions inside the nanoparticles. At the same time, PSer-*b*-PGlu nanoparticles exhibit significantly higher D_H in weakly alkaline buffer solution compared to deionized water. This may be due to the higher ionization of the PGlu block and the repulsion of uniformly charged polymer chains. As expected, the hydrodynamic diameter for the charged self-assembled soft nanoparticles is at least twice as large as their average diameter determined in the dry state using TEM.[15,17] This fact can be explained by the depletion of the hydration shell and the collapse of charged polymer chains upon drying. Thus, the obtained nanoparticles can be classified as nanogels formed as a result of the physical self-assembly of functional polypeptides.[18]

Drug loading and encapsulation efficiency were determined by varying the initial DOX content from 200 to 1000 μg mg^{-1} nanoparticles (Table S2). For both types of nanoparticles, encapsulation is high and ranges from 85 to 97% for P(Glu-*co*-Phe) and from 93 to 99% for PSer-*b*-PGlu. This high drug loading is attributed to ionic interactions and hydrogen bonds between the γ-carboxyl groups of glutamic acid in the copolymers and the amino group, as well as the numerous hydroxyls of DOX. In addition, hydrophobic interactions may also play a role in loading DOX into P(Glu-*co*-Phe) nanoparticles. To evaluate the physicochemical characteristics, samples of P(Glu-*co*-Phe) and PSer-*b*-PGlu nanoparticles containing 459 ± 15 μg DOX mg^{-1} and 490 ± 10 μg DOX mg^{-1}, respectively, were selected. DOX encapsulation resulted in a slight decrease in hydrodynamic diameters and an increase in polydispersity index (PDI) and zeta potential (see Table 1). Several factors can lead to such results. For both polypeptides, self-assembly of nanoparticles occurs, the structure of which is not fixed, but flexible and sensitive to interactions with other components. Therefore, drug loading can affect the reorganization and packing density of nanoparticles depending on the drug–polymer interaction. Hydrophobic interactions, most pronounced when DOX is loaded into P(Glu-*co*-Phe), lead to densification of the nanoparticles. This results in a decrease in both the hydrodynamic diameter (DLS) and the average diameter ($\bar{D}$) determined by the TEM method. In turn, DOX loading into PSer-*b*-PGlu is supported mainly by hydrogen bonding and ionic interactions, since this copolymer lacks a sufficient fraction of hydrophobic moiety. As a result, these nanoparticles have a looser structure, which allows drug uptake with a less pronounced change in hydrodynamic diameter.

The functional property of potential delivery systems, such as the rate of drug release in different media, is very important, since the drug release profile determines the frequency of administration of the nanoformulation. The release of DOX from polypeptide

† Nanoparticle dispersions were prepared by simply redispersing lyophilized copolymers in deionized water or 0.1 M phosphate-buffered saline (PBS, a phosphate buffer solution containing 0.9% NaCl) at concentrations of 1–5 mg ml^{-1} under short-term sonication (30 s).

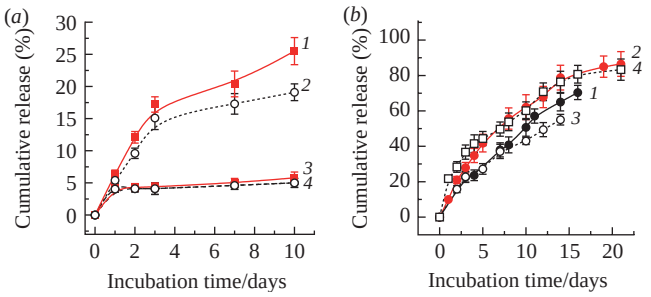

Figure 2 DOX release profiles in different media and at different DOX loadings: (*a*) release from (*1*),(*3*) PSer-*b*-PGlu and (*2*),(*4*) P(Glu-*co*-Phe) in (*1*),(*2*) 0.1 M sodium phosphate buffer (pH 5.0) and (*3*),(*4*) 0.1 M PBS (pH 7.4) at a DOX load of 278 ± 12 μg mg^{-1} nanoparticles; (*b*) release from (*1*),(*2*) PSer-*b*-PGlu and (*3*),(*4*) P(Glu-*co*-Phe) in blood plasma at a DOX load of (*1*),(*3*) 278 ± 12 μg mg^{-1} nanoparticles and (*2*),(*4*) 982 ± 11 μg mg^{-1} nanoparticles. The standard deviation does not exceed 10% of the mean.

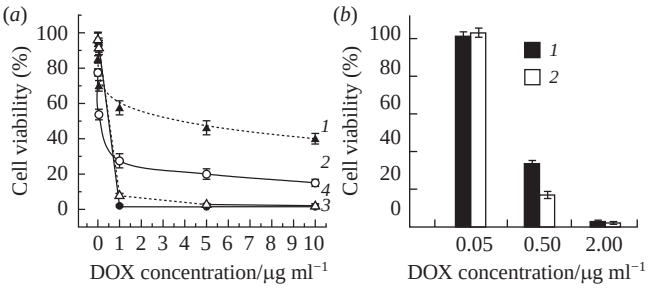

Figure 3 Viability of MCF-7 and A431 cells at various DOX concentrations. (*a*) Incubation of MCF-7 cells with (*1*)–(*3*) P(Glu-*co*-Phe)/DOX and (*4*) PSer-*b*-PGlu/DOX for (*1*) 24, (*2*) 48 and (*3*),(*4*) 96 h. (*b*) Incubation of A431 cells with (*1*) PSer-*b*-PGlu and (*2*) P(Glu-*co*-Phe) nanoparticle formulations for 72 h.

nanoparticles was studied in two buffer media with pH 7.4 and pH 5.0, simulating the pH of blood and tumor tissue, respectively, as well as in blood plasma. Figure 2(*a*) shows that the release of DOX from both nanoformulations occurs more intensely in an acidic environment. Specifically, 17–25% of DOX is released at pH 5.0 *versus* 5% at pH 7.4. This result is consistent with previously published data on the release of DOX from PEG-*b*-PGlu[19] and PEG-*b*-PGlu/Ca[20] nanoparticles. Due to the presence of γ-carboxylic groups with pK_a ~4.3, PGlu is a pH-sensitive polymer, protonation of which in acidic media reduces drug retention by the polymer, which in turn promotes more pronounced drug release.

However, the most pronounced release of DOX was found in plasma, which is a complex biological fluid containing enzymes and proteins [Figure 2(*b*)]. In this case, the release reached 55 and 70% for P(Glu-*co*-Phe) and PSer-*b*-PGlu, respectively. The slower release of DOX from the P(Glu-*co*-Phe)-based delivery system may be due to the presence of a hydrophobic moiety that better retains DOX compared to the hydrophilic PSer-*b*-PGlu. Note that the release of DOX depends not only on the medium, its composition and pH, but also on the initial loading. Indeed, in the case of the polypeptide nanoparticles under study, the release was more pronounced with increasing load [see Figure 2(*b*)]. At load values differing by a factor of 3.5, the release of DOX into the blood plasma increases by 15 and 30% in the case of PSer-*b*-PGlu and P(Glu-*co*-Phe), respectively.

Before an *in vivo* experiment, it is recommended to study the *in vitro* cytotoxicity of any biomaterials. For instance, Le *et al.* recently reported the correlation of *in vitro* cytotoxicity studies with *in vivo* results.[21] The authors observed that the cytotoxicity of DOX against 4T1 breast cancer cells was consistent with tumor growth suppression in 4T1-bearing mice *in vivo*.

In this work, both the cytotoxicity of empty nanoparticles and the inhibitory activity of their DOX-containing formulations were evaluated in MCF-7 (human breast adenocarcinoma) and A431 (human epidermoid carcinoma) cancer cells. The viability of MCF-7 cells as a function of the concentration of DOX loaded into the nanoparticles and their contact time is shown in Figure 3(*a*). Even at minimal concentrations, DOX in different nanoparticles killed cancer cells upon prolonged interaction. Dose-dependent inhibition of cancer cells for both kinds of DOX nanoformulations was also observed for A431 cancer cells [Figure 3(*b*)], whereas empty carriers showed no cytotoxicity to them. Optical microscopy images of A431 cells demonstrating the effects of different concentrations of DOX are shown in Figure S4.

In addition, the time stability of both DOX nanoformulations was tested in a complex biological medium such as Dulbecco's Modified Eagle Medium (DMEM). P(Glu-*co*-Phe)/DOX nanoparticles were found to be stable after incubation at 37 °C for 4 days. In turn, the PGlu-*b*-PSer/DOX nanoformulation quickly aggregates in DMEM culture medium under the same conditions (Figure S5). This result can be explained by better stabilization of amphiphilic P(Glu-*co*-Phe) nanoparticles due to hydrophobic interactions of Phe units. Considering these results, more stable P(Glu-*co*-Phe)-based DOX nanoformulations were selected for further *in vivo* studies.

In this work, the efficacy and tolerability of therapy using DOX delivery systems at doses exceeding the maximum tolerated dose (MTD) were studied in *in vivo* experiments on transgenic FVB/N mice. FVB/N is a transgenic mouse line that overexpresses HER-2/neu proteins and serves as a model for breast cancer research.[22] These mice are characterized by the development of spontaneous mammary adenocarcinomas in females. In males, tumors arise in 100% of cases as a result of tumor cell transplantation.[22]

The P(Glu-*co*-Phe)/DOX nanoformulation at a total dose of 10 mg per mouse was administered subcutaneously to mice in the experimental group,‡ while mice in the control group were not subjected to chemotherapy. P(Glu-*co*-Phe)/DOX was administered as a double injection of single doses of 5 mg per mouse. The second dose was administered 21 days after the first injection. In this case, the total dose of DOX exceeded the MTD of DOX by 38 times. As already noted, free DOX, when administered subcutaneously or intramuscularly, causes tissue damage and necrosis. Comparative photographs of animals one week after subcutaneous administration of 10 mg per mouse of the DOX nanoformulation and free DOX are shown in Figure S6. After subcutaneous injection of the DOX nanoformulation, no necrotic changes were observed. For details on examining mice and sampling liver and subcutaneous tissue at the injection site for histological examination, see Online Supplementary Materials.

The median life expectancy in the control group was 61.5 days, while in the experimental group it was 81 days ($p \leqslant 0.01$) (Figure S7). The tumor volumes of mice in the control and experimental groups were 13 ± 4 and 5 ± 2 cm^3, respectively. The antitumor effect of the tested formulation can be characterized by tumor growth inhibition (GI) and efficacy index (EI) values (see Online Supplementary Materials), which were found to be GI = 65.3% and EI = 2.9. A morphological examination of animal livers revealed vacuolar dystrophy of hepatocytes as a manifestation of DOX hepatotoxicity. The reversibility of toxic manifestations was evidenced by the absence of vacuolar dystrophy, starting from 61 days after administration of the DOX nanoformulation.

‡ The experimental group consisted of five male animals. Males were previously transfected with a mammary adenocarcinoma tumor from females onto the outer surface of the pelvic limb. All procedures with animals complied with the ethical standards approved by the Russian Federation State Standard (no. 33216-2014) and the principles of the Basel Declaration.

In summary, the polypeptides P(Glu-*co*-Phe) and PSer-*b*-PGlu were synthesized, which form spherical nanoparticles with high DOX loading capacity. It was shown that, in contrast to PSer-*b*-PGlu, P(Glu-*co*-Phe) nanoparticles retain their hydrodynamic diameter in a complex biological medium for several days. In various media, sustained release of DOX was demonstrated *in vitro*, which was enhanced in acidic buffer solution and blood plasma. The polypeptide nanoparticles were found to be nontoxic to cancer cells, while their DOX nanoformulations exhibited dose-dependent inhibition of cell growth. *In vivo* experiments on transgenic FVB/N mice showed that the P(Glu-*co*-Phe)-based DOX nanoformulation when administered subcutaneously at a dose exceeding the MTD does not induce damage and necrosis of epidermal tissue. Moreover, the developed nanoformulation provides a cytostatic effect and effectively controls tumor growth.

This work was performed within the framework of State Assignments of the Institute of Macromolecular Compounds RAS and the Ministry of Health of the Russian Federation. HPLC-MS and TEM analyses were carried out at the Chemical Analysis and Materials Research Center and the Center for Molecular and Cell Technologies of the Research Park of Saint-Petersburg State University with the support of project no. 075-15-2021-637.

Online Supplementary Materials

Supplementary data associated with this article can be found in the online version at doi: 10.1016/j.mencom.2024.01.006.

References

1 B. S. Chhikara and K. Parang, *Chem. Biol. Lett.*, 2023, **10**, 451.
2 E. Alphandéry, *J. Cancer*, 2014, **5**, 472.
3 B. Gao, J. Luo, Y. Liu, S. Su, S. Fu, X. Yang and B. Li, *Int. J. Nanomed.*, 2021, **16**, 4073.
4 G. Minotti, P. Menna, E. Salvatorelli, G. Cairo and L. Gianni, *Pharmacol. Rev.*, 2004, **56**, 185.
5 J. Liu, S. Li, J. Wang, N. Li, J. Zhou and H. Chen, *Recent Pat. Anti-Cancer Drug Discovery*, 2023, **18**, 125.
6 T. Wen, A. Yang, L. Piao, S. Hao, L. Du, J. Meng, J. Liu and H. Xu, *Int. J. Nanomed.*, 2019, **14**, 4475.
7 L. Tang, W. Jiang, L. Wu, X. Yu, Z. He, W. Shan, L. Fu, Z. Zhang and Y. Zhao, *Int. J. Nanomed.*, 2021, **16**, 7875.
8 D. Matyszewska, *Surf. Innovations*, 2014, **2**, 201.
9 E. Pedziwiatr-Werbicka, K. Horodecka, D. Shcharbin and M. Bryszewska, *Curr. Med. Chem.*, 2021, **28**, 346.
10 V. V. Spiridonov, A. R. Lukmanova, D. V. Pozdyshev, A. A. Markova, Y. L. Volodina, G. V. Golovina, V. V. Shakhmatov, V. A. Kuzmin, V. I. Muronetz and A. A. Yaroslavov, *Mendeleev Commun.*, 2023, **33**, 553.
11 A. M. Demin, A. V. Vakhrushev, M. S. Valova, M. A. Korolyova, M. A. Uimin, A. S. Minin, K. A. Chistyakov, V. P. Krasnov and V. N. Charushin, *Mendeleev Commun.*, 2023, **33**, 160.
12 Z. Li, S. Tan, S. Li, Q. Shen and K. Wang, *Oncol. Rep.*, 2017, **38**, 611.
13 N. N. Sudareva, O. M. Suvorova, E. G. Korzhikova-Vlakh, I. I. Tarasenko, K. A. Kolbe, N. V. Smirnova, N. N. Saprykina and D. N. Suslov, *Tech. Phys.*, 2022, **67**, 277 (*Zh. Tekh. Fiz.*, 2022, **92**, 933).
14 C. Oussoren, W. M. C. Eling, D. J. A. Crommelin, G. Storm and J. Zuidema, *Biochim. Biophys. Acta, Biomembr.*, 1998, **1369**, 159.
15 N. N. Sudareva, O. M. Suvorova, I. I. Tarasenko, N. N. Saprykina, N. V. Smirnova, S. G. Petunov, A. S. Radilov, A. S. Timin, E. G. Korzhikova-Vlakh and A. D. Vilesov, *Mendeleev Commun*., 2020, **30**, 25.
16 N. N. Zashikhina, D. V. Yudin, I. I. Tarasenko, O. M. Osipova and E. G. Korzhikova-Vlakh, *Polym. Sci., Ser. A*, 2020, **62**, 43 (*Vysokomol. Soedin., Ser. A*, 2020, **62**, 46).
17 N. Zashikhina, V. Sharoyko, M. Antipchik, I. Tarasenko, Y. Anufrikov, A. Lavrentieva, T. Tennikova and E. Korzhikova-Vlakh, *Pharmaceutics*, 2019, **11**, 27.
18 S. Hajebi, N. Rabiee, M. Bagherzadeh, S. Ahmadi, M. Rabiee, H. Roghani-Mamaqani, M. Tahriri, L. Tayebi and M. R. Hamblin, *Acta Biomater.*, 2019, **92**, 1.
19 L. Zhang, P. Zhang, Q. Zhao, Y. Zhang, L. Cao and Y. Luan, *J. Colloid Interface Sci.*, 2016, **464**, 126.
20 K. Li, D. Li, L. Zhao, Y. Chang, Y. Zhang, Y. Cui and Z. Zhang, *Bioact. Mater.*, 2020, **5**, 721.
21 A. N. Stukov, S. F. Vershinina, N. A. Koziavin, T. Yu. Semiglazova, L. V. Filatova, D. Kh. Latipova, A. O. Ivantsov, V. G. Bespalov, A. L. Semenov, O. A. Belyaeva, G. S. Kireeva, V. A. Alexandrov, G. V. Tochilnikov, I. N. Vasilyeva, M. A. Maydin, M. L. Tyndyk, S. S. Kruglov, G. A. Yanus and M. N. Yurova, *Siberian Journal of Oncology*, 2019, **18** (5), 54.
22 W. J. Muller, J. Ho and P. M. Siegel, *Biochem. Soc. Symp.*, 1998, **63**, 149.

Received: 9th August 2023; Com. 23/7222